

**SERDP POLLUTION PREVENTION**

**PROJECT PP 1150**

**ELECTRODEPOSITED MN-SN-X ALLOYS  
FOR CORROSION PROTECTION COATINGS**

Giovanni Zangari

Department of Metallurgical and Materials Engineering  
University of Alabama  
Tuscaloosa AL 35487-0202

**FINAL TECHNICAL REPORT SEPTEMBER 30, 2002**

# Report Documentation Page

Form Approved  
OMB No. 0704-0188

Public reporting burden for the collection of information is estimated to average 1 hour per response, including the time for reviewing instructions, searching existing data sources, gathering and maintaining the data needed, and completing and reviewing the collection of information. Send comments regarding this burden estimate or any other aspect of this collection of information, including suggestions for reducing this burden, to Washington Headquarters Services, Directorate for Information Operations and Reports, 1215 Jefferson Davis Highway, Suite 1204, Arlington VA 22202-4302. Respondents should be aware that notwithstanding any other provision of law, no person shall be subject to a penalty for failing to comply with a collection of information if it does not display a currently valid OMB control number.

1. REPORT DATE <b>30 SEP 2002</b>		2. REPORT TYPE		3. DATES COVERED <b>00-00-2002 to 00-00-2002</b>	
4. TITLE AND SUBTITLE <b>Electrodeposited Mn-Sn-X Alloys for Corrosion Protection Coatings</b>				5a. CONTRACT NUMBER	
				5b. GRANT NUMBER	
				5c. PROGRAM ELEMENT NUMBER	
6. AUTHOR(S)				5d. PROJECT NUMBER	
				5e. TASK NUMBER	
				5f. WORK UNIT NUMBER	
7. PERFORMING ORGANIZATION NAME(S) AND ADDRESS(ES) <b>University of Alabama, Department of Metallurgical and Materials Engineering, Tuscaloosa, AL, 35487-0202</b>				8. PERFORMING ORGANIZATION REPORT NUMBER	
9. SPONSORING/MONITORING AGENCY NAME(S) AND ADDRESS(ES)				10. SPONSOR/MONITOR'S ACRONYM(S)	
				11. SPONSOR/MONITOR'S REPORT NUMBER(S)	
12. DISTRIBUTION/AVAILABILITY STATEMENT <b>Approved for public release; distribution unlimited</b>					
13. SUPPLEMENTARY NOTES					
14. ABSTRACT					
15. SUBJECT TERMS					
16. SECURITY CLASSIFICATION OF:			17. LIMITATION OF ABSTRACT	18. NUMBER OF PAGES	19a. NAME OF RESPONSIBLE PERSON
a. REPORT <b>unclassified</b>	b. ABSTRACT <b>unclassified</b>	c. THIS PAGE <b>unclassified</b>			

## 1. BACKGROUND AND TECHNICAL APPROACH

Electrodeposited cadmium (Cd) is extensively used in numerous applications for defense finishing requirements, such as coatings providing sacrificial corrosion protection, low coefficient of friction, and/or good solderability. One main drawback of Cd and Cd processing however are their extreme toxicity to the environment and to humans. A number of alternatives to Cd have been developed for definite applications, but no substitute is at present completely satisfactory for any single application, where the customer has come to expect all the advantages of Cd: sacrificial protection, limited formation of corrosion scales, good lubricity, pleasant appearance, solderability, and conductivity.

Electrodeposited coatings of manganese (Mn) or Mn-alloys potentially combine good sacrificial corrosion protection with adequate tribological behavior and suitable mechanical properties for coating steel products. Although pure manganese can provide excellent sacrificial protection for steel, it is highly chemically reactive and might not survive prolonged exposure when immersed in an electrolyte or exposed outdoors. Alloying Mn with a nobler metal can however reduce its reactivity. An additional drawback of electrodeposited manganese or some Mn alloys is that they undergo phase transformation in several weeks at room temperature, from the ductile  $\gamma$  form (body centered tetragonal, bct), to the  $\alpha$  brittle form (body centered cubic, bcc), which induces deterioration of the coatings' mechanical properties.

Sn and Sn alloys have also been extensively studied and used as protective coatings, due to their outstanding nontoxicity, corrosion resistance, low friction coefficient and solderability. Electrodeposited Sn-Mn coatings are thus of great interest, as they potentially combine the barrier properties of tin with the sacrificial protection afforded by manganese. Cu-Mn alloys are also of interest, as it is known that the addition of 2-3% Cu to Mn coatings stabilizes the ductile form of Mn.

## 2. OBJECTIVE

This project seeks to develop novel, low cost, and environmentally benign electrodeposition processes for the production of alloy coatings based on Mn and/or Sn, which combine high corrosion protection performance, good tribological behavior, and suitable mechanical properties, that would thus constitute realistic alternatives to cadmium.

On the basis of the discussion in section 1, we are seeking in particular to study in detail the electrodeposition of Sn-Mn and Cu-Mn binary alloys. The microstructure, chemical, electrochemical and physical properties, tribological and mechanical characteristics, as well as corrosion resistance of these coatings are also investigated.

## 3. DELIVERABLES

Deliverables in this project include electrodeposition processes for the production of Mn based coatings with the potential to exhibit high corrosion protection performance combined with good tribological behavior, as well as a database of the properties of such alloys.

## 4. PROJECT ACCOMPLISHMENTS

### A. Mn electrodeposition [1]

As a starting point in the development of viable processes for the electrodeposition of various Mn alloys, the electrodeposition of Mn from ammonium sulfate electrolytes in the pH range 1.7-7.5 and current density from 30 to 330 mA/cm<sup>2</sup> is studied. Morphological, chemical, structural characterization and open circuit potential measurements in solution were further used to characterize the properties of the deposits. In order to attempt stabilization of the ductile  $\gamma$  manganese form, the phase transformation kinetics and their dependence on current density and pH were investigated. This part of the work provides a range of processing conditions for the production of high quality Mn deposits.

Manganese was electrodeposited galvanostatically at room temperature from simple sulfate solutions with the formulation MnSO<sub>4</sub> 0.59M + (NH<sub>4</sub>)<sub>2</sub>SO<sub>4</sub> 1M. Current density (CD) was varied from 30 to 330 mA/cm<sup>2</sup>. No stirring was employed. From 30 to 100 mA/cm<sup>2</sup>, silver-gray, dense, uniform films with well developed crystallites (type I) were formed. Black, shining films with a cellular microstructure (type II) were instead grown at current density above 150 mA/cm<sup>2</sup> (Figure 1).

X-ray diffraction (Figure 2) shows that the type I deposit is pure  $\gamma$ -Mn (fcc) and type II is amorphous. Upon aging for several days at room temperature, the ductile  $\gamma$ -Mn gradually transforms to brittle  $\alpha$ -Mn (Figure 3). The rate of transformation approximately follows a Johnson-Mehl-Avrami behavior.

The two different microstructures I and II exhibit a different chemical stability in various corrosive environments. Plots of corrosion potential  $E_{\text{corr}}$  vs. time for manganese electrodeposited at different current densities in different corrosion systems shows that amorphous coatings have better corrosion resistance in H<sub>3</sub>BO<sub>3</sub>+Na<sub>2</sub>SO<sub>4</sub> solutions, while crystalline coatings show improved performance in NaCl solutions.

Manganese was electrodeposited at pH varying in the range 1.8 to 7.0. From Figure 4 and 5, it can be seen that pH has a strong effect on the texture of the deposits obtained. At pH from 2 to 3, an in-plane preferential orientation along (002) is identified, while at higher pH no texture is observed. Plating at pH ranging from 2 to 6 does not influence to any relevant extent the corrosion resistance of Mn deposits.

### B. Sn-Mn electrodeposition [2]

Pure Mn is strongly chemically reactive and a coating of this material may provide sacrificial protection only for a limited time when immersed in an electrolyte or exposed outdoors. Tin and tin alloys on the other hand are well known for their stability in various environment, due to the formation of a thin, stable oxide layer. In addition, Sn coatings have been studied as protective coatings, due to their outstanding nontoxicity, corrosion resistance, low friction coefficient and solderability. Electrodeposited tin-manganese coatings are thus of great interest, as they potentially combine the barrier properties of tin with the sacrificial protection afforded by manganese. In this section, an electrochemical investigation of Sn-Mn ammonium sulfate electrolytes with and without additives is conducted, and the results are used to prepare coatings of Sn-Mn under different deposition conditions. The morphology, crystal structure and corrosion

resistance of the resulting coatings are thus evaluated, and the various electrolyte chemistries are compared.

The addition of ammonium sulfate polarizes the  $\text{Sn}^{2+}$  discharging potential to a more negative value (about  $-0.6 \text{ V}_{\text{SCE}}$ ) while shifting the  $\text{H}^+$  and  $\text{Mn}^{2+}$  reduction reactions to more positive potentials, thus bringing the reduction potentials of Sn and Mn closer. This makes codeposition of Sn and Mn possible, even if Sn still deposits preferentially and Mn codeposition is always accompanied by hydrogen evolution (Figure 6).

Sn-Mn deposits were grown galvanostatically from ammonium sulfate solutions with or without additives at a temperature of  $25 \text{ }^\circ\text{C}$ , with the current density varying in the range 10 to  $600 \text{ mA/cm}^2$  at pH 2.5-3.0. Sn-Mn coatings obtained from simple ammonium sulfate baths at low current density contain a large amount of tin and oxygen and exhibit a heterogeneous microstructure (Figure 7, left). These coatings are generally heterogeneous, containing various Sn-Mn intermetallic structures, as well as Sn, Mn and their oxides. On the contrary, at high current density, sound and homogeneous Sn-Mn coatings can be synthesized which contain metallic Mn and a small amount of tin and oxygen (Figure 7, right), and possess an amorphous structure.

The addition of tartrate, EDTA or gluconate suppresses Mn reduction and thus increases Sn content in the coatings. Correspondingly, the coatings appearance and microstructure at low current density is improved, yielding more compact and homogeneous morphologies (Figure 8).

Sn-Mn coatings show an anodic potentiodynamic behavior intermediate between that of pure manganese and pure tin (Figure 9), probably due to their heterogeneity. Their electrochemical characteristics can consequently be adjusted by varying alloy composition and structure (Figure 10). Coatings with high percentage of intermetallic  $\text{Mn}_{1.77}\text{Sn}$  phase have best sacrificial protection for steel.

### C. Cu-Mn electrodeposition [3, 4]

Due to its high chemical reactivity and brittle nature, pure manganese has not been considered suitable as a protective coating for steel. In section 3 it has been shown that the first problem can be overcome by codepositing Mn with nobler metals such as Sn. However, either pure manganese or the Sn-Mn alloys have been found to undergo a phase transformation at room temperature in a time frame of a few weeks, from the ductile  $\gamma$  form (body centered tetragonal, bct), to the brittle  $\alpha$  form (body centered cubic, bcc), which induces a deterioration of the coatings' mechanical properties. This phase transformation is undesirable and should be prevented or retarded.

It has been reported that the codeposition of copper, a face centered cubic (fcc) metal, with  $\gamma$ -manganese (body centered tetragonal, bct, also called distorted fcc) can stabilize manganese in its ductile form. In this section, an electrochemical investigation of a Cu-Mn alloy electrodeposition bath based on ammonium sulfate, at pH 6.4-6.6 and 2.6-2.8, and at different cupric ion concentrations is conducted by using cathodic potentiodynamic and cyclic voltammetry methods. Galvanostatic electrodeposition is used to grow Cu-Mn coatings from different baths and at different current density and pH. Morphological, chemical, structural, tribological, mechanical characterization and electrochemical corrosion measurements were further used to characterize the properties of the deposits. The phase transformation kinetics is also monitored qualitatively. This provides a detailed study on the electrodeposition of high quality Cu-Mn alloy coatings

with different properties, which may be further utilized in the development of environmentally friendly ternary Cu-Mn-X alloys (X = Sn, Zn, Ni, Co, Fe, Bi) with desirable physical and electrochemical properties.

Figure 11 shows the cathodic potentiodynamic behavior of  $\text{MnSO}_4 + (\text{NH}_4)_2\text{SO}_4$  solutions with and without  $\text{CuSO}_4$  (0.005 M), at different pH. The solution containing  $\text{CuSO}_4$  at pH 2.6-2.8 shows four main reactions: moving from noble to active potentials these are respectively the reduction of  $\text{Cu}^{2+}$ ,  $\text{H}_3\text{O}^+$ ,  $\text{H}_2\text{O}$ , and  $\text{Mn}^{2+}$ .

It can be seen that as pH increases, the rate of the  $\text{H}_3\text{O}^+$  reduction decreases to a low value and its discharging characteristic cannot be discerned from the curves. In addition, the discharge potential for  $\text{H}_2\text{O}$  reduction shifts cathodically, which can be attributed to the decrease of  $[\text{H}^+]$ . Figure 12 shows that with the increase of  $[\text{Cu}^{2+}]$ , the limiting current density for  $\text{Cu}^{2+}$  discharge increases correspondingly.

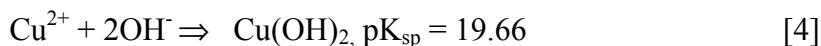
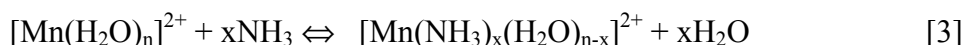
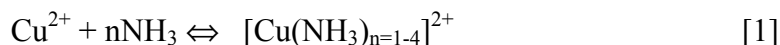
Cu-Mn deposits were grown galvanostatically from electrolytes containing only ammonium sulfate as an additive at a temperature of 25 °C, with current density varying in the range from 50 to 600  $\text{mA}/\text{cm}^2$ , pH 2.6-2.8 or 6.4-6.6. SEM micrographs of Cu-Mn coatings electrodeposited at different current densities from electrolytes containing  $\text{CuSO}_4$  0.005 M,  $\text{MnSO}_4$  0.59 M and  $(\text{NH}_4)_2\text{SO}_4$  1 M at pH 2.6-2.8 are shown in Figure 13. The composition determined by EDX shown below each micrograph is the relative atomic ratio of copper and manganese. Current densities less than 150  $\text{mA}/\text{cm}^2$  can only yield dark and porous coatings, with high oxygen content. A transition of the film microstructure from porous and spongy to dense and crystalline (type I) also occurs at higher current densities, and the films obtained at 150  $\text{mA}/\text{cm}^2$  show transitional characteristics. From 150 to 330  $\text{mA}/\text{cm}^2$ , regular type I coatings can be grown, with little variation in microstructure and chemical composition. No oxygen is incorporated in Type I films. The composition of each coating is compared with that of the corresponding films grown at pH 6.4-6.6 in Figure 14. Upon further raising the current density, a new type of coating forms, which has a compact, uniform, glossy and bright metal appearance and is called type II in the following discussion. In addition to copper and manganese, type II coatings also contain a considerable amount of oxygen. In appearance and microstructure, Cu-Mn type II coatings resemble the amorphous manganese and Sn-Mn coatings produced at high current density, which contain hydrated oxides of manganese.

XPS depth profiling reveals that copper exists in its metallic form in both types of electrodeposited Cu-Mn coatings. For type I films, the Mn:O:Cu atomic ratio changes from 31:66:3 at the surface (after etching 5 cycles, about 10 nm) to 91:6:3 in the interior (after etching 60 cycles, about 120 nm). Type I coatings can thus be considered a metallic film with an oxide surface. For type II coatings, the Mn:O:Cu atomic ratio changes from 61:36:3 at 10 nm depth to 90:7:3 at 120 nm depth. This compositional variation for type II Cu-Mn coatings is different from that of pure Mn coatings, where the composition and chemical states of Mn do not depend on depth, and Mn is predominantly in the +2 and +3 valence states. The oxygen inclusions are in the form of  $\text{MnO}_x(\text{OH})_{2-x}\cdot n\text{H}_2\text{O}$ , where x increases and n decreases with depth.

The effect of the variation of cupric ion concentration ( $[\text{Cu}^{2+}]$ ) on the electrodeposition process and the coating properties have been studied at low pH (2.6-2.8). The optimal current density ranges for producing type I and II coatings are strongly dependent on  $[\text{Cu}^{2+}]$ , and this dependence is shown in Figure 15. An increase of  $[\text{Cu}^{2+}]$

widens the current density range where porous coatings are produced, and increases the current density necessary to obtain type I and II coatings.

From the results shown above, it can be concluded that the introduction of cupric sulfate, though in a small amount, changes coating properties and optimal electrodeposition conditions as a consequence of variations in bath chemistry. At low current density, manganese deposition rate is low, compared with the galvanic corrosion rate. Therefore, manganese is difficult to deposit. As hydrogen evolution always occurs, the pH in the vicinity of the cathode increases, but probably not to such extent that the free  $\text{NH}_3$  can complex all  $\text{Cu}^{2+}$ . Increasing current density induces a larger pH excursion on the cathode surface, thus producing more  $\text{NH}_3$ . Non-complexed  $[\text{Cu}^{2+}]$  can be reduced to such a low level that no  $\text{Cu}(\text{OH})_2$  can be formed. Relevant reactions and equilibria are listed below.



At low current density, the local pH is comparatively stable due to chemical equilibria established between  $\text{H}_2\text{O}$ ,  $\text{NH}_3$ ,  $\text{Cu}^{2+}$  and  $\text{Mn}^{2+}$ , so manganese hydroxide(s) cannot be formed and crystalline Cu-Mn coatings of good quality and coverage can be deposited. At higher current densities however,  $[\text{OH}^-]$  in the vicinity of the cathode may increase beyond the buffering ability of  $(\text{NH}_4)_2\text{SO}_4$  and  $\text{Cu}^{2+}$ , and  $\text{Mn}(\text{OH})_2$  would be formed and incorporated into the films. Under these conditions, type II coatings would be obtained. The distribution of the various complexes at different pH is calculated and shown in Figure 16.

The cross-section of the type I Cu-Mn coatings was also studied by SEM and EDX. Figure 17 shows the cross-sectional views of a  $\text{Cu}_4\text{Mn}_{96}$  crystalline (type I) coating obtained from a bath containing  $\text{MnSO}_4$  (0.59 M),  $(\text{NH}_4)_2\text{SO}_4$  (1 M) and  $\text{CuSO}_4$  (0.005 M) at  $200 \text{ mA/cm}^2$  and pH 2.6-2.8. Composition on both sides was studied by EDX and XPS depth profiling. Type I coatings are shown to have a Cu rich interface with the substrate, composed of very small grains.

X-ray diffraction was performed to determine the crystal structure of the as-deposited coatings. Figure 18 shows the XRD patterns ( $\theta$ - $2\theta$  scans) of as-deposited Cu-Mn alloy coatings obtained at different current densities, pH 2.6-2.8. Almost no signal from the deposit can be detected by XRD when the deposition current density is less than  $100 \text{ mA/cm}^2$ . This is consistent with the coating appearance and SEM micrographs. Crystalline  $\gamma$ -manganese phase coatings (type I) are observed for samples obtained above  $150 \text{ mA/cm}^2$ , while no fcc copper peaks could be found. This result shows that the Cu-Mn high temperature solid solution ( $\gamma$ -phase) is formed by electrodeposition. As current density increases over  $400 \text{ mA/cm}^2$ , the (200) and (002) diffraction peaks are weakened,

while the (111) peak becomes broader, indicating a decrease in grain size or a transition to an amorphous structure (type II), which is also confirmed by the observed variation of microstructure with current density.

The effect of sample aging at room temperature on the crystal structure of Cu-Mn alloy coatings with different composition, obtained from a low pH bath containing different  $[\text{Cu}^{2+}]$ , was studied by X-ray diffraction. The diffraction patterns of as-deposited coatings and those after 8 months aging at room temperature are shown in Figure 19. Copper in solid solution is able to greatly retard the precipitation of room temperature equilibrium  $\alpha$ -manganese (bcc) from the high temperature  $\gamma$ -phase (fct). A higher copper content tends to increase the lattice  $c/a$  ratio and preserve the high temperature  $\gamma$ -phase for a longer time. The coatings with a copper content of more than 3.8 at. % maintain the  $\gamma$ -phase for more than 8 months.

Mechanical and tribological properties have been tested, and the results are shown in Table 1 and compared with those of electrodeposited Cd and Mn. Hardness was measured with a Hysitron nanomechanical properties system, and a Nano Indenter II system was used to perform constant load nanoscratch test and evaluate the friction coefficients. Force-displacement curves determined by nano-hardness measurements are shown in Figure 20.

The corrosion resistance of Cu-Mn coatings was studied by anodic polarization in 3% NaCl at pH 3.0. The results for typical Cu-Mn coatings are compared to Cu and Mn in figure 21, and the behavior of Cu-Mn coatings with different compositions is shown in figure 22. For both types of pure manganese, a maximum active current region ( $0.01\text{-}0.1\text{ A/cm}^2$ ) extends from  $-1.2$  to  $-0.1\text{ V}_{\text{SCE}}$ , and subsequently a decrease of current density about one order of magnitude occurs, probably due to the accumulation of corrosion products ( $\text{MnO}_x\text{OH}_{2-x}$ ,  $x = 0 \sim 2$ ) on the specimen. The corrosion potential ( $E_{\text{corr}}$ ) and current ( $I_{\text{corr}}$ ) were evaluated using the Stern-Geary equation. Codeposition of copper causes a higher  $I_{\text{corr}}$  and a more positive  $E_{\text{corr}}$  than pure Mn. A barrier or passive behavior was observed at  $-0.5 \sim 0.1\text{ V}_{\text{SCE}}$ .

For a better understanding of the passivity of electrodeposited Cu-Mn coatings, SEM, XRD and XPS analyses of Cu-Mn coatings were carried out after anodic potentiodynamic polarization. Figure 23 shows the surface morphology of two types of Cu-Mn coatings after anodic polarization from a potential cathodic with respect to  $E_{\text{corr}}$  up to 0.5 V. The apparent compositions determined by EDX analysis are  $\text{Cu}_5\text{Mn}_{31}\text{O}_{64}$  (type I) (Figure 23(a)) and  $\text{Cu}_{12}\text{Mn}_{26}\text{O}_{62}$  (type II) (Figure 23(b)). In both cases, no substrate area is exposed as evidenced by EDX. The attack seems to be uniform, especially for amorphous coatings (type II). The observed microcracks might be due to internal stresses present in the as-deposited films. Compared with the as-deposited composition, manganese content decreases due to its preferential oxidation and dissolution in corrosive media. XRD analysis (Figure 24) reveals that in addition to the  $\gamma$ -phase Cu-Mn peaks, some broad peaks are detected for the corroded sample surface. This is due to the complex nature of the corrosion products. Detailed investigation shows that a mixture of Mn(II) to Mn(IV) oxides (mainly  $\text{MnO}_2$ ) is the most probable substance present on the specimen surface. During the anodic polarization process,  $\text{Mn}(\text{OH})_2$  and  $\text{MnO}_2$  are progressively formed, which are stable in chloride solutions.  $\text{Cu}_2\text{O}$  also forms but it is not protective in chloride environments.

## 5. CONCLUSIONS

Sn-Mn alloy coatings can combine the sacrificial behavior of Mn with the protection afforded by Sn. However, coatings are often heterogeneous and their corrosion performance is probably limited by the formation of corrosion couples. In fact, coatings with a high percentage of the intermetallic  $Mn_{1.77}Sn$  offer the best corrosion behavior.

Cu-Mn coatings with appropriate composition on the other hand combine stability of the ductile crystalline structure with the capability of forming a partially protective layer to slow down alloy corrosion. In addition, the tribological properties of Cu-Mn coatings appear comparable, if not superior, to those of cadmium. However, the corrosion resistance of Cu-Mn is still not comparable to that of Cd reference films, and further improvements in alloy formulation might be needed. A possible route towards further improvements of these alloys is the investigation of ternary Cu-Mn-Sn coatings of suitable composition. Although difficult to synthesize in a reliable manner, the potential characteristics of these alloys warrant further research.

## 6. TRANSITION PLAN AND RECOMMENDATION

The performance of binary alloys as ascertained from laboratory tests is very encouraging. Further development of the electrodeposition process to warrant predictable properties and uniform coverage of irregular parts however is required. In addition, field tests of the coatings should be performed to ascertain their performance under realistic service conditions.

Further development of this class of alloys can be achieved by investigating ternary alloys as suggested in the Conclusion section. The possibility of combining the sacrificial properties of Mn with the stability provided by Cu and the tribological properties and protection afforded by Sn could yield coatings which would constitute a realistic alternative to Cd.

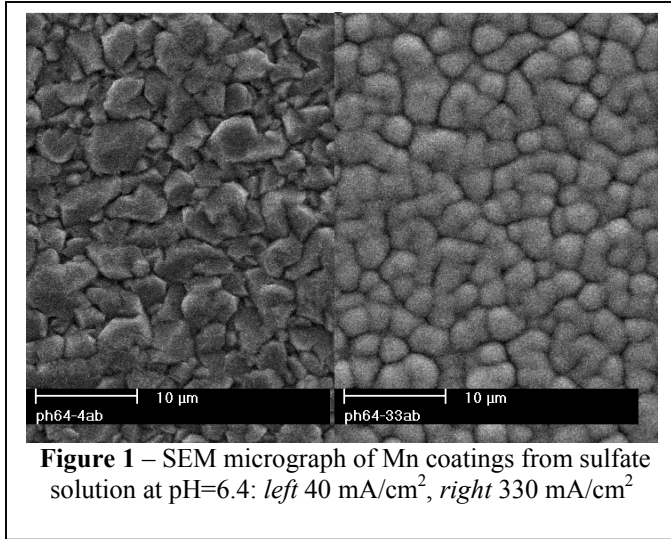
## REFERENCES AND PUBLICATIONS RESULTING FROM THIS WORK

[1] J. Gong and G. Zangari "Electrodeposition and characterization of Manganese coatings" J. electrochem. Soc. 149 (4) C209 (2001).

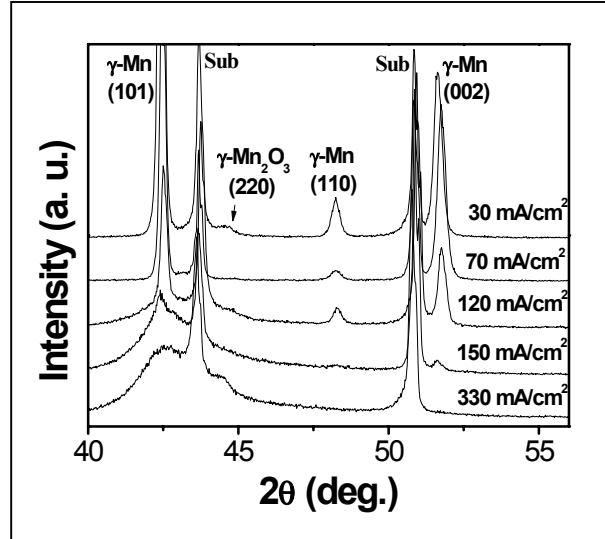
[2] J. Gong, G. Zangari "Electrodeposition of sacrificial tin-manganese alloy coatings" Mat. Sci. Eng. A, to be published (2002)

[3] J. Gong, G. Zangari "Electrodeposition and characterization of sacrificial copper-manganese alloy coatings. Part I: electrochemical deposition and structural characterization", J. electrochem. Soc., submitted.

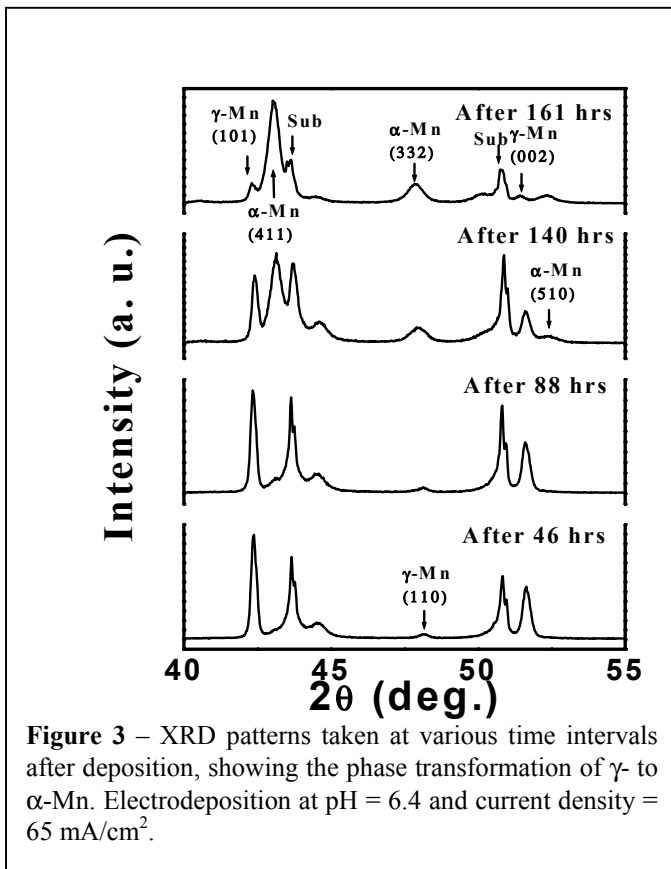
[4] J. Gong, G. Zangari "Electrodeposition and characterization of sacrificial copper-manganese alloy coatings. Part II: corrosion resistance and structural characterization", J. electrochem. Soc., submitted.



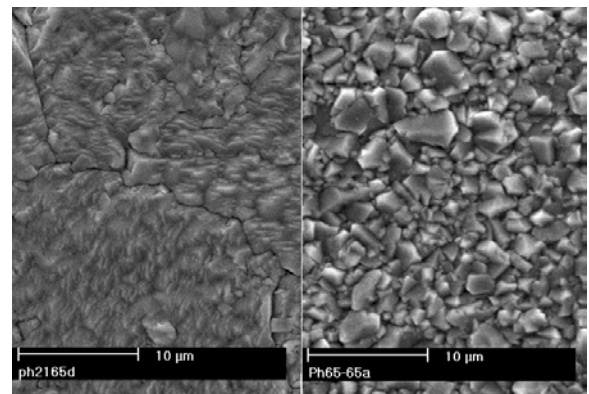
**Figure 1** – SEM micrograph of Mn coatings from sulfate solution at pH=6.4: *left* 40 mA/cm<sup>2</sup>, *right* 330 mA/cm<sup>2</sup>



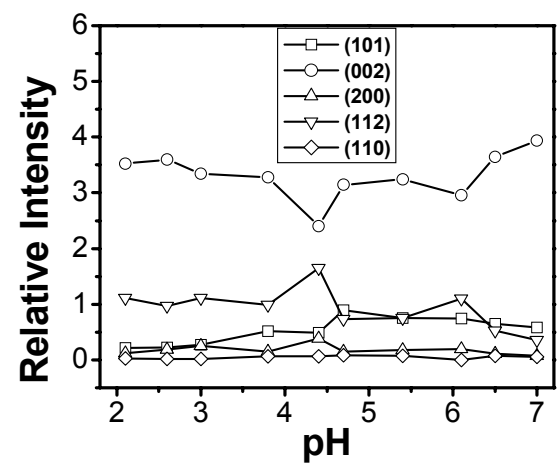
**Figure 2** – XRD patterns of as-deposited Mn films at pH = 6.4. Note the broadening of the  $\gamma$ -Mn diffraction peaks with increasing current density.



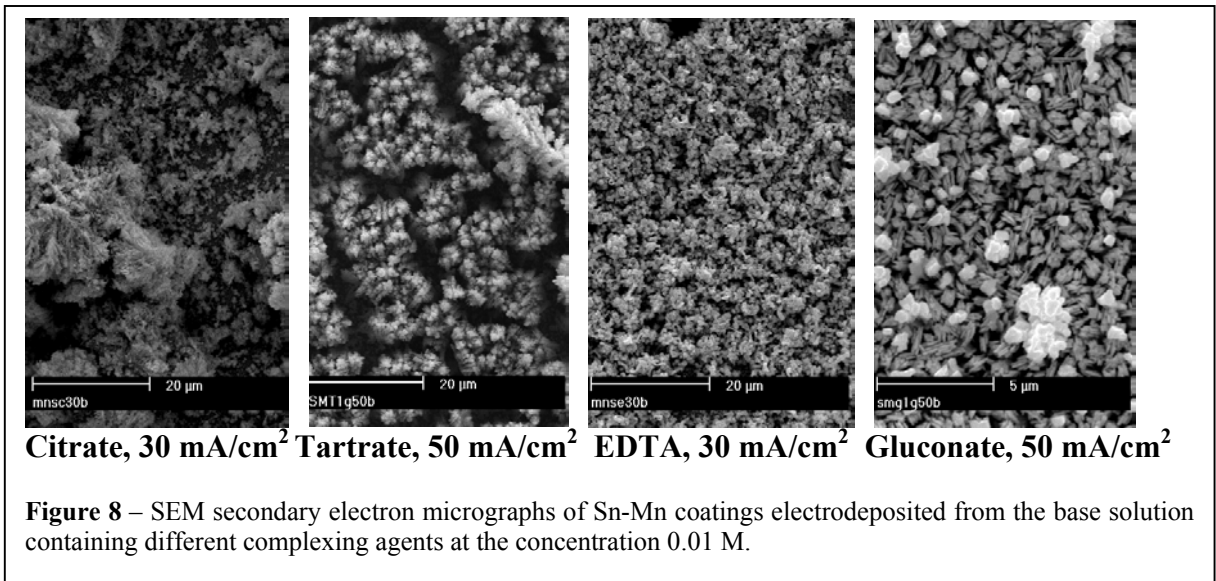
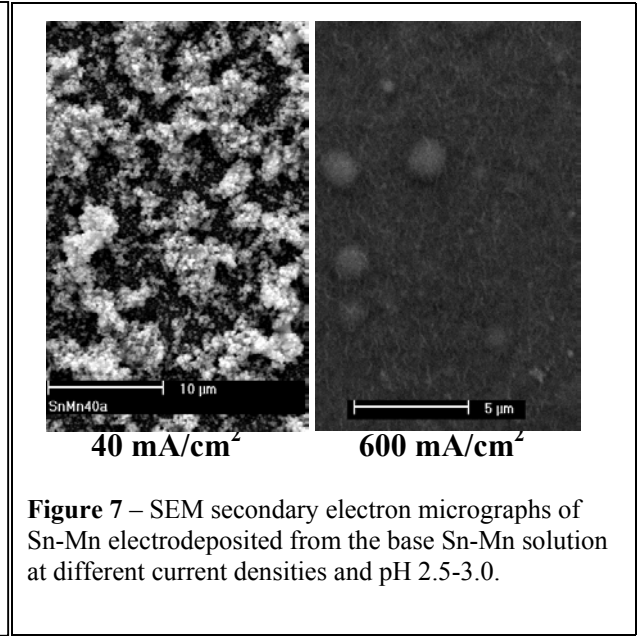
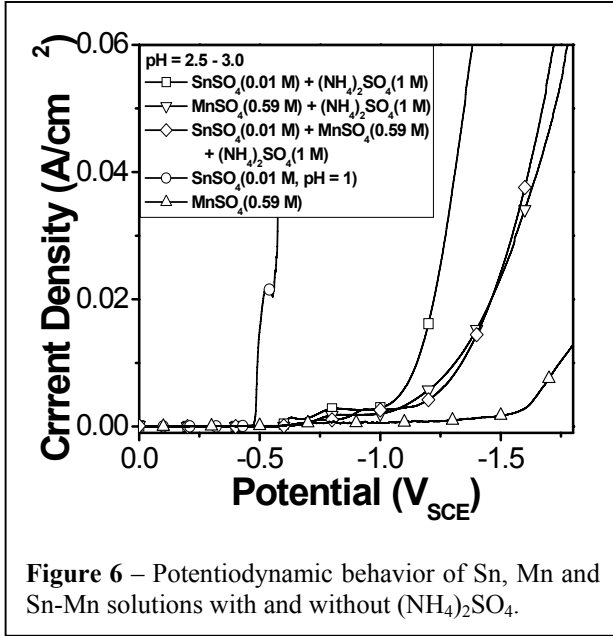
**Figure 3** – XRD patterns taken at various time intervals after deposition, showing the phase transformation of  $\gamma$ - to  $\alpha$ -Mn. Electrodeposition at pH = 6.4 and current density = 65 mA/cm<sup>2</sup>.

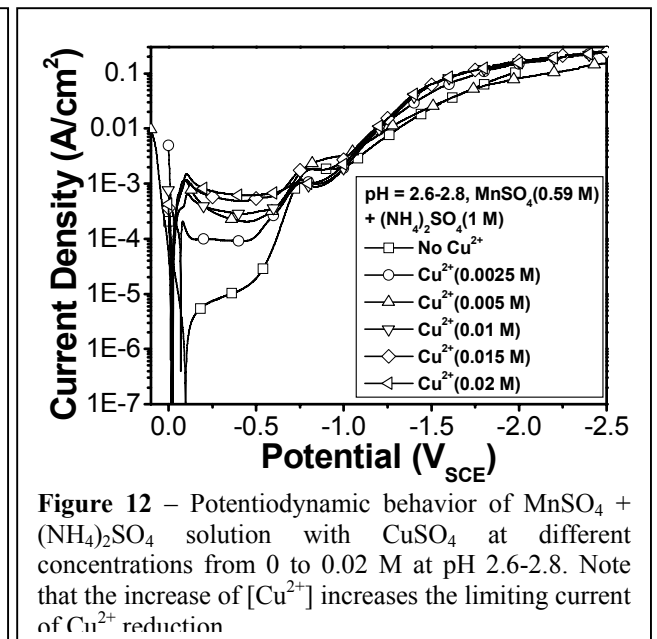
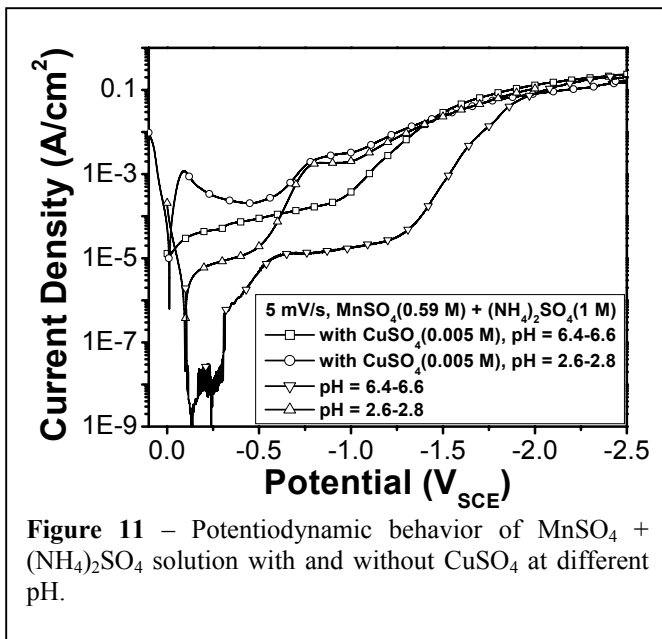
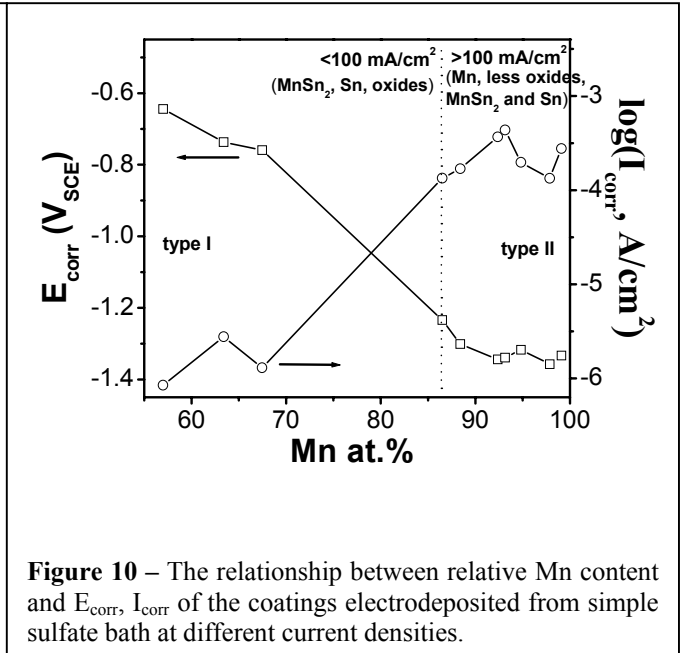
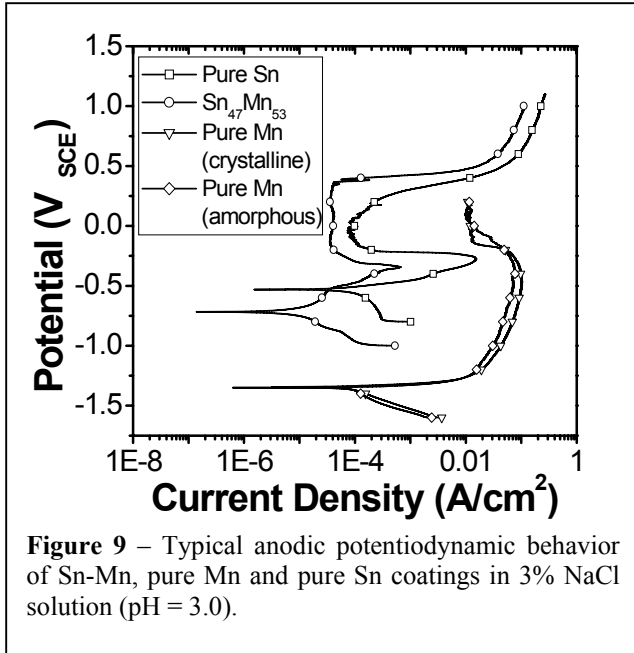


**Figure 4** - SEM micrograph of Mn coatings from sulfate solution at the CD of 65 mA/cm<sup>2</sup>: *left* pH=2.1, *right* pH=6.5



**Figure 5** – Relative integrated intensities of the diffraction peaks for as-deposited  $\gamma$ -Mn as a function of pH.





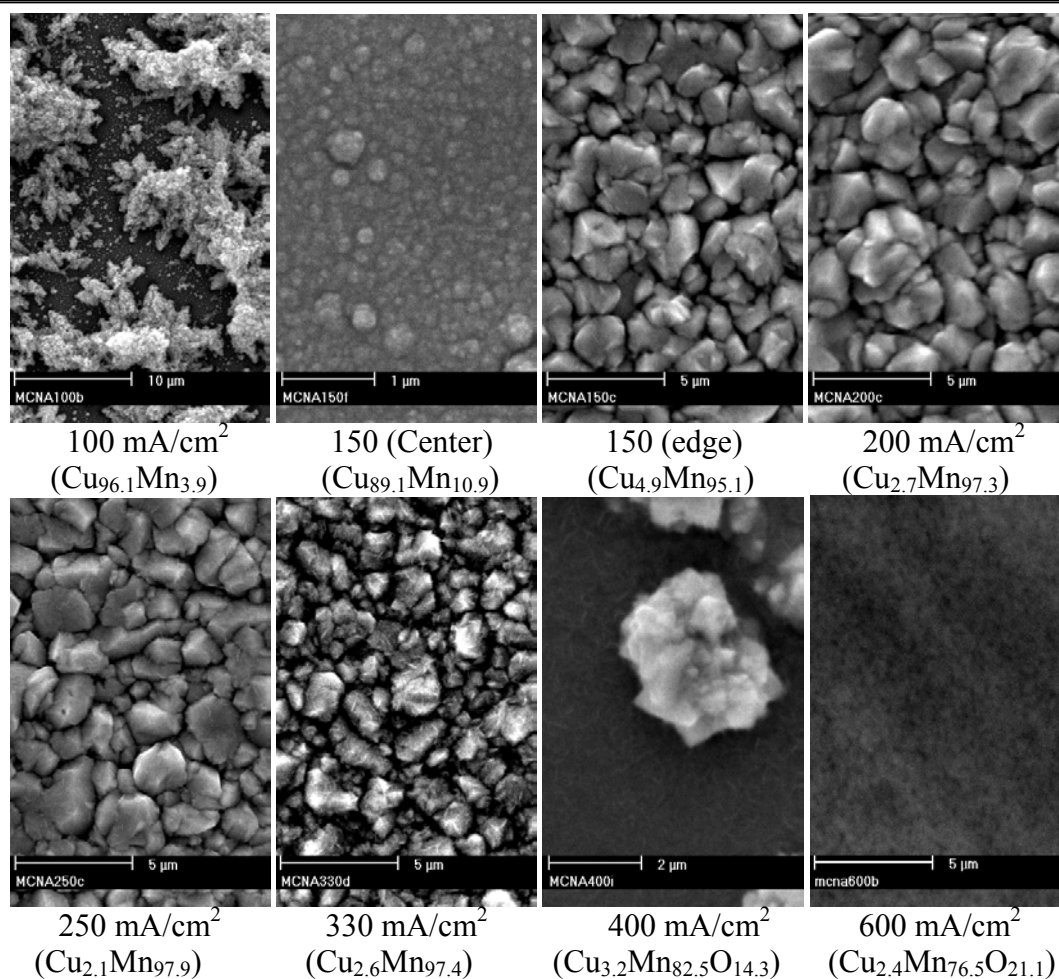


**Figure 13** – SEM secondary electron surface micrographs of Cu-Mn coatings electrodeposited at various current densities at pH 2.6-2.8. The data below each image are respectively the current density and the coating composition. (c) – (f) are type I coatings and (h) is type II coating.

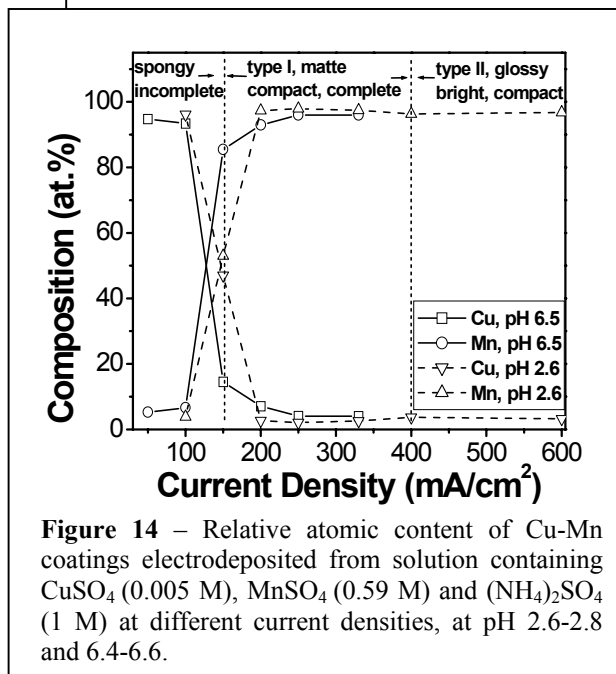


**Figure 14** – Relative atomic content of Cu-Mn coatings electrodeposited from solution containing CuSO<sub>4</sub> (0.005 M), MnSO<sub>4</sub> (0.59 M) and (NH<sub>4</sub>)<sub>2</sub>SO<sub>4</sub> (1 M) at different current densities, at pH 2.6-2.8 and 6.4-6.6.

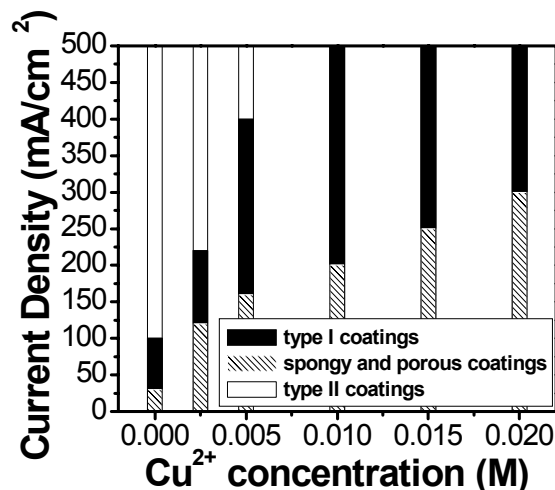
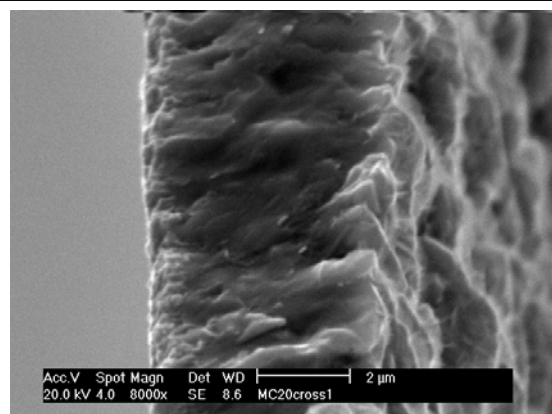
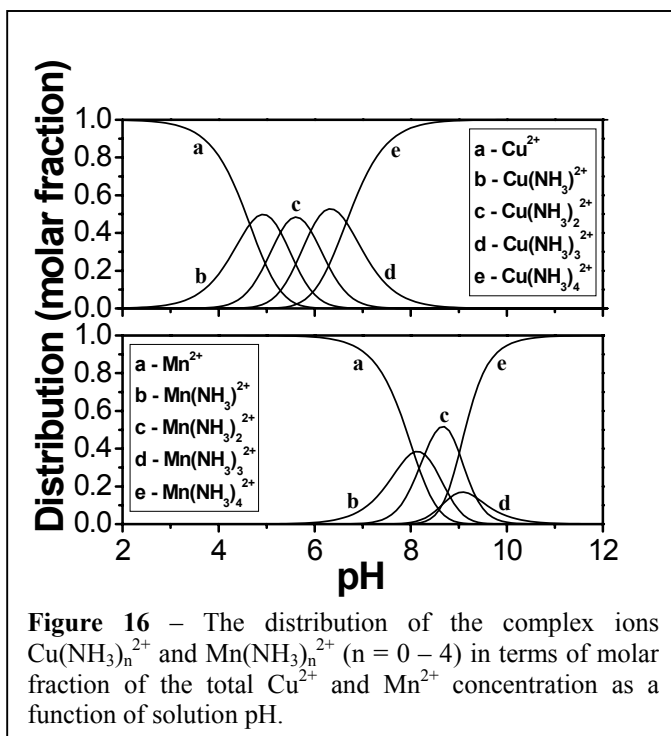
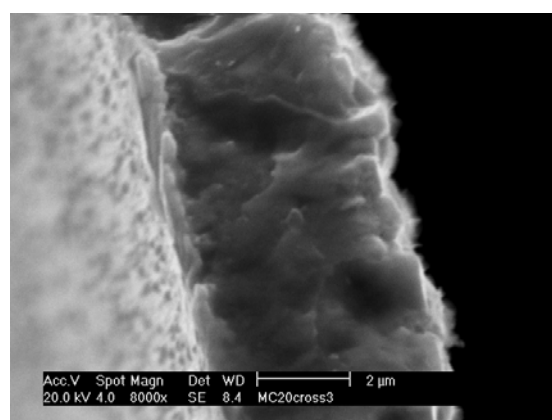


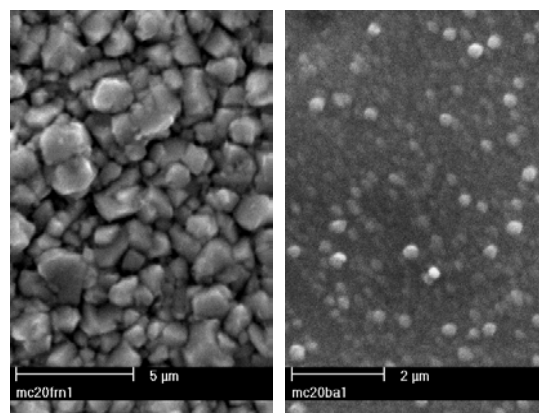
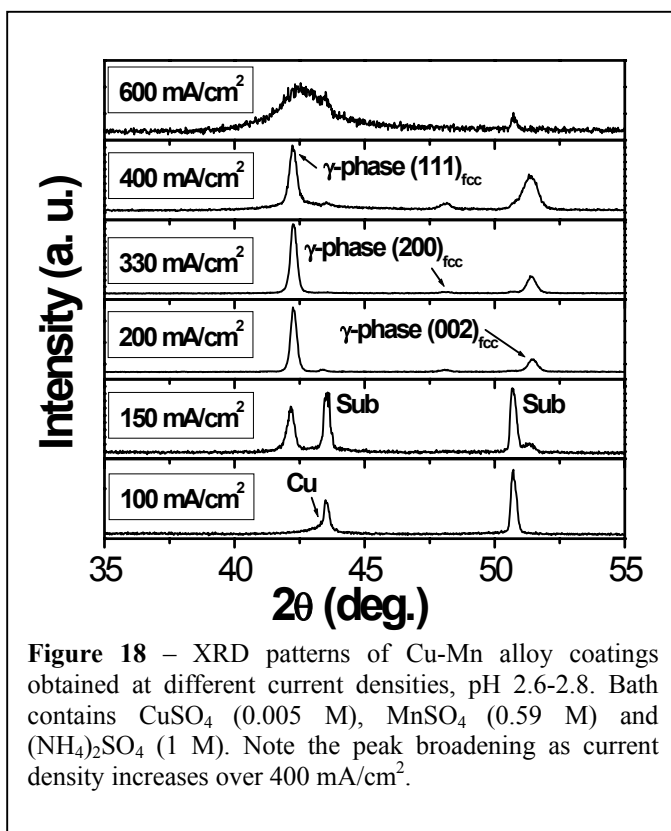
**Figure 15** – The effect of cupric ion concentration in Cu-Mn plating electrolytes on the optimal current density range to produce different types of coatings. In addition to CuSO<sub>4</sub>, all electrolytes contain MnSO<sub>4</sub> (0.59 M) and (NH<sub>4</sub>)<sub>2</sub>SO<sub>4</sub> (1 M), pH 2.6-2.8.



(a) cross-section (front side)



(b) cross-section (backside)



(c) front side (d) backside

**Figure 17** – SEM secondary electron micrographs of (a) front side cross-section, (b) backside cross-section, (c) front side surface and (d) backside surface of a  $\text{Cu}_{4.07}\text{Mn}_{95.93}$  film obtained from a bath containing  $\text{MnSO}_4$  (0.59 M),  $(\text{NH}_4)_2\text{SO}_4$  (1 M) and  $\text{CuSO}_4$  (0.005 M) at pH 2.6-2.8 and current density  $200 \text{ mA/cm}^2$ .

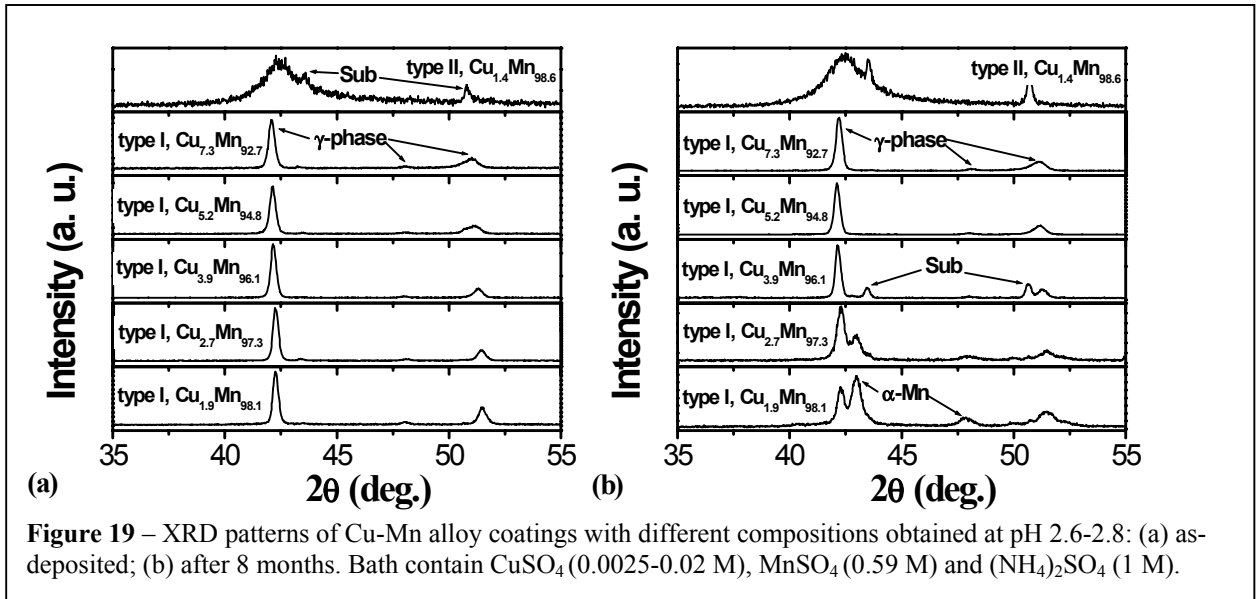
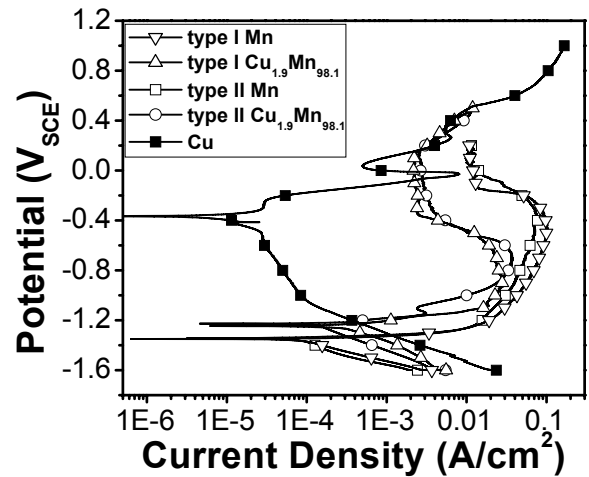
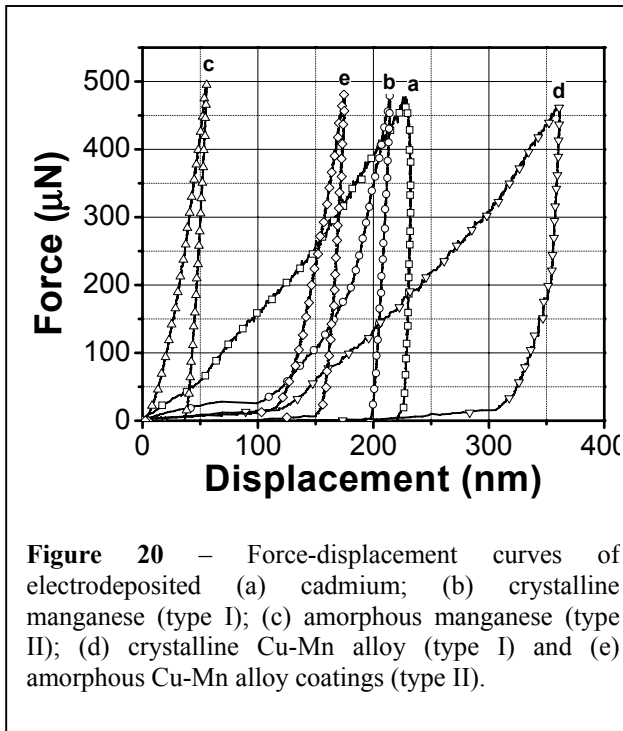
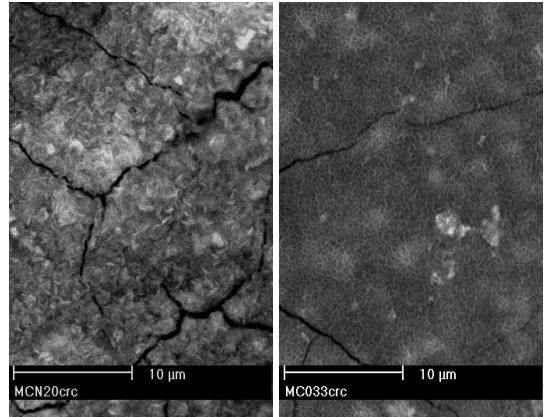
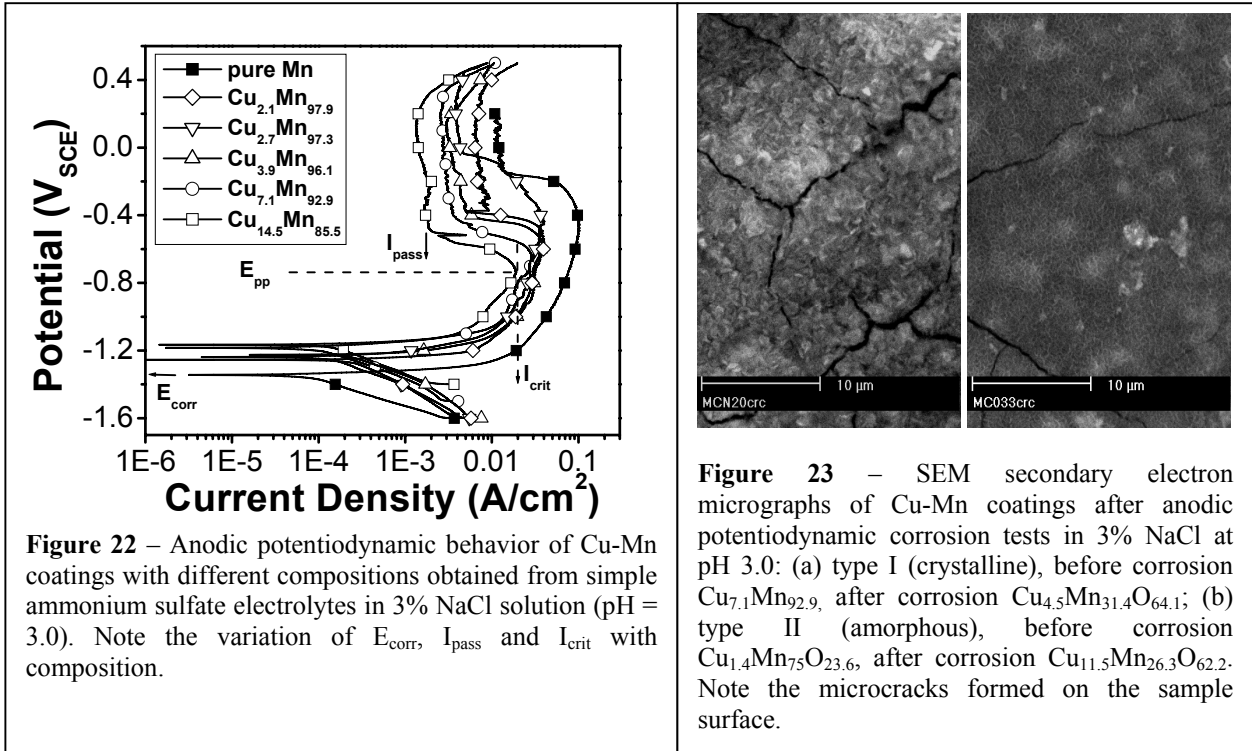


Table 1 – Mechanical and tribological properties of ECDCu-Mn coatings

	ECD Cd	Type I Mn	Type II Mn	Type I Cu-Mn	Type II Cu-Mn
Friction Coefficient	0.8	/	0.5	0.7	0.5
Nanohardness H (GPa)	0.3	0.4	4.0	0.1	0.5
Reduced modulus E <sub>r</sub> (GPa)	151.9	31.1	95.3	10.5	32.9





**Figure 23** – SEM secondary electron micrographs of Cu-Mn coatings after anodic potentiodynamic corrosion tests in 3% NaCl at pH 3.0: (a) type I (crystalline), before corrosion  $Cu_{7.1}Mn_{92.9}$ , after corrosion  $Cu_{4.5}Mn_{31.4}O_{64.1}$ ; (b) type II (amorphous), before corrosion  $Cu_{1.4}Mn_{75}O_{23.6}$ , after corrosion  $Cu_{11.5}Mn_{26.3}O_{62.2}$ . Note the microcracks formed on the sample surface.

